

Vacancy concentrations in noncubic metals. Lattice constants of zinc*†

Michael Current[‡] and H. M. Gilder[§]

Physics Department, Rensselaer Polytechnic Institute, Troy, New York 12181

(Received 26 August 1976; revised manuscript received 19 May 1977)

Measurements of the thermal expansion of the lattice parameters of Zn are combined with earlier measurements of the bulk expansion of oriented single-crystal bars to give a measure of the fraction of vacant lattice sites at temperatures near the melting point. The vacancy fraction at the melting point, $\eta(T_m)$, is $(3.0 \pm 1.0) \times 10^{-4}$, and the single-vacancy formation parameters are energy of formation $E^f = 0.52 \pm 0.05$ eV, and entropy of formation $S^f = (0.5 \pm 0.3)k$. The strains associated with dislocation climb in response to changing vacancy concentrations favor dilation perpendicular to the c axis. A comparison is made of the principal-axis strains in noncubic metals as measured by thermal expansion and vacancy-flux electromigration methods.

I. INTRODUCTION

Since the early work by Feder and Nowick¹ with Al, the direct comparison of precision measurements of bulk and lattice-parameter thermal expansion has been used to determine the concentrations of point defects in nearly a dozen metals.² While most of the studies have been made on fcc and bcc lattice structures, results on vacancy concentrations have been obtained for a number of axial crystals, Cd,^{3,4} Mg,⁵ Sn,^{6,7} and Zn.⁷

The difference between the bulk and lattice-parameter volume dilations gives the net change in the number of lattice sites in a crystal resulting from the formation of lattice defects,

$$\left(\frac{\Delta v}{v_0}\right)_{\text{bulk}} - \left(\frac{v}{v_0}\right)_{x \text{ ray}} = (\eta_{\text{vac}} + 2\eta_{\text{divac}} + \dots) - \eta_{\text{int}}, \quad (1)$$

where $(\Delta v/v_0)_{\text{bulk}}$ and $(\Delta v/v_0)_{x \text{ ray}}$ are the volume dilation of the bulk and x-ray lattice cell, respectively, v_0 is a reference volume at a temperature where the defect effects are negligible, and η_{vac} , η_{divac} , and η_{int} are the fractions of vacancies, divacancies, and interstitials present in the crystal. This difference is independent of the relaxations of the lattice around the defect.^{8,9}

In crystals with axial symmetry, the volume dilation is a sum of the linear dilations along the principal symmetry directions, so

$$\left(\frac{\Delta v}{v_0}\right)_{\text{bulk}} \equiv (\Delta l/l_0)_c + (2\Delta l/l_0)_a \quad (2)$$

and

$$\left(\frac{\Delta v}{v_0}\right)_{x \text{ ray}} \equiv \Delta c/c_0 + 2\Delta a/a_0,$$

where l_c and l_a are the macroscopic linear dimensions and a and c are the lattice parameters for the cell directions perpendicular and parallel to the axial direction. With the convenient definitions,

$$\Delta_a \equiv (\Delta l/l_0)_a - \Delta a/a_0 \quad (3)$$

and

$$\Delta_c \equiv (\Delta l/l_0)_c - \Delta c/c_0$$

the defect population is given by

$$\Delta_c + 2\Delta_a = (\eta_{\text{vac}} + 2\eta_{\text{divac}} + \dots) - \eta_{\text{int}}. \quad (4)$$

The quantity Δ_a/Δ_c is a measure of the anisotropy of the strains arising from the dislocation climb processes associated with the generation and annihilation of defects within the crystal.¹⁰ An anisotropy in these strains ($\Delta_a/\Delta_c \neq 1$) would also appear in vacancy flux electromigration measurements in oriented single crystals.

II. EXPERIMENT

Measurements of the bulk thermal expansion of Zn by Gilder and Wallmark¹¹ were made by monitoring the motion of the surface indent markers near the ends of a $15 \times 1 \times 1$ cm single-crystal bar. Special care was taken to establish isothermal conditions during each marker-location measurement. An absolute temperature determination was made with an NBS standard Pt-10-at.-%-Rh thermocouple (which was also used in the x-ray measurements). The temperature variations in all cases were kept to less than 0.15°C .

The lattice parameter measurements were made in a modified Bond apparatus¹² built for Dr. R. Feder of IBM-Yorktown Heights. With a Hilger and Watts model TB 95/5 precision clinometer, the orientation of the crystal mount shaft could be directly monitored to $1''$ of arc. The angular width of the $\text{Cu } K\alpha_1$ peak was of the order of $5'$ arc and the center line of the peak could usually be determined to within $3''$ of arc. For each measurement, two resonance reflection conditions were obtained by rotating the central shaft perpendicular to the incoming x-ray beam. The differ-

ence between the shaft positions at resonance, ΔR , is related to the Bragg angle, θ_B by

$$\theta_B = \frac{1}{2}\pi - \frac{1}{2}\Delta R. \quad (5)$$

The (006) and (210) reflections were used to measure the dilations of the c - and a -lattice parameters, respectively. Prior to each run, the furnace core was evacuated with a mechanical pump and then filled with a slight positive pressure of He. This procedure was used to establish convective thermal contact with furnace walls while minimizing the risk of problems with oxidation or vaporization at high temperatures.

The crystals were grown in the form of 1-cm-diam rods from 99.999%-pure Commenco stock in a Bridgman furnace. The rods were then sliced into 1-cm lengths with an acid-etching saw. Laue back-reflection photographs were used to check the quality of the lattice and to aid in the alignment of the crystal in the furnace. After an initial annealing period at $\sim 400^\circ\text{C}$, the crystals were followed through heating and cooling cycles over the course of several weeks.

III. RESULTS

The percent changes in the axial and basal lattice parameters of Zn are listed in Tables I and II. The a -axis data are taken from the work of S. Apostolu.¹³ The reference lattice parameters (not corrected for refraction) are c_0 (47.9°C) = 4.9538 \AA and a_0 (46.2°C) = 2.6652 \AA . The wavelength of the $\text{Cu } K\alpha_1$ line was taken to be 1.54051 \AA .¹⁴ In the range from room temperature up to within $\sim 100^\circ\text{C}$ of the melting point, these changes are coincident with the bulk-dilation measurements of Gilder and Wallmark. The clear increase in the bulk dilation over the lattice parameter expansion above 300°C (see Fig. 1-3) is an indication of the addition of lattice sites to the crystal which results from the generation of additional vacancies as the temperature of the crystal is raised.

The principal-axis differences, Δ_a and Δ_c , as well as the net fraction of vacant lattice sites, $\eta(T) = 2\Delta_a + \Delta_c$, are displayed in Fig. 4. While the dilation in the c -axis direction is approximately three times the dilation in the basal direction, the difference between the bulk and lattice expansion has the opposite sense ($\Delta_a/\Delta_c \sim 1.5$). The temperature variation of $\eta(T)$ gives a monovacancy-formation energy of $E^f = 0.52 \pm 0.05 \text{ eV}$. The vacancy fraction at the melting point is $(3 \pm 1.0) \times 10^{-4}$. The entropy associated with changes in the lattice-vibration frequencies is $S^f = (0.5 \pm 0.3)k$.

TABLE I. c -axis lattice parameter thermal expansion of zinc.

Heating T ($^\circ\text{C}$)	$10^5\Delta_c/c_0$	Cooling T ($^\circ\text{C}$)	Run $10^5\Delta_c/c_0$
31.7	-99.2	19.5	-180.1
40.0	-48.0	34.7	-81.0
47.9	0	47.9	0
62.4	95.9	56.1	49.8
80.0	206.5	71.0	143.4
92.6	288.7	93.0	277.0
113.1	416.7	114.5	416.1
127.8	501.9	130.5	518.5
148.8	634.0	150.6	640.0
174.4	804.9	176.8	800.0
196.3	939.8	193.9	909.7
209.1	1012.0	208.7	1000.4
225.5	1111.0	225.9	1108.0
239.6	1198.0	238.5	1185.0
263.7	1345.0	245.3	1232.0
279.2	1438.0	265.2	1352.0
291.7	1515.0	278.6	1431.0
307.9	1609.0	293.6	1524.0
327.5	1720.0	308.2	1607.0
346.0	1833.0	317.5	1659.0
361.8	1917.0	331.8	1741.0
371.0	1965.0	345.7	1820.0
376.0	1986.0	354.9	1875.0
382.2	2018.0	361.1	1910.0
387.9	2053.0	367.6	1942.0
392.9	2077.0	373.5	1975.0
396.7	2097.0	379.0	2003.0
403.1	2128.0	384.0	2032.0
408.8	2155.0	389.7	2064.0
414.0	2182.0	395.0	2086.0
		400.6	2115.0
		408.1	2151.0

TABLE II. a -axis lattice parameter thermal expansion of zinc.

T ($^\circ\text{C}$)	$10^4\Delta_a/a_0$	T ($^\circ\text{C}$)	$10^4\Delta_a/a_0$
46.2	0	355.1	55.675
51.6	0.810	360.4	56.949
73.4	3.650	371.4	59.723
93.4	6.442	379.7	61.693
109.6	9.031	383.0	62.947
123.8	11.131	383.8	62.894
145.8	14.375	384.3	63.027
174.1	18.980	391.2	65.055
191.0	22.056	392.0	65.242
208.0	24.823	396.3	66.337
239.0	30.922	399.5	67.407
262.4	35.175	399.6	67.406
291.1	41.017	404.0	68.637
302.6	43.398	404.2	68.743
322.9	48.150	406.8	69.386
339.7	51.935	407.4	69.815
341.2	52.150	410.7	70.135

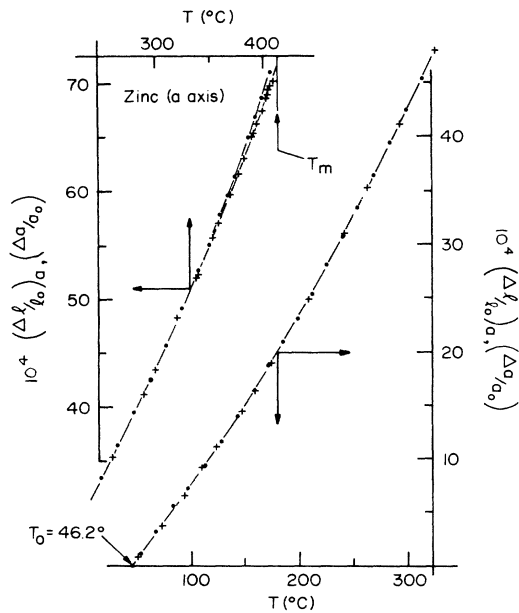


FIG. 1. Bulk (●) and lattice parameter (+) dilation for the basal direction in Zn.

IV. DISCUSSION

A. Energy of formation

The present result for E^f is in close agreement with the value of 0.54 ± 0.02 eV which follows from studies of the variation of positron lifetimes in Zn with temperature.¹⁵ The change in the positron

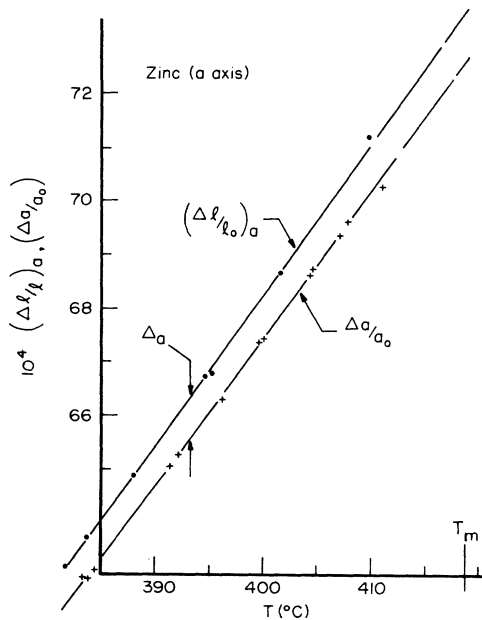


FIG. 2. Bulk (●) and lattice parameter (+) dilation for the basal direction in Zn at temperatures approaching the melting point.

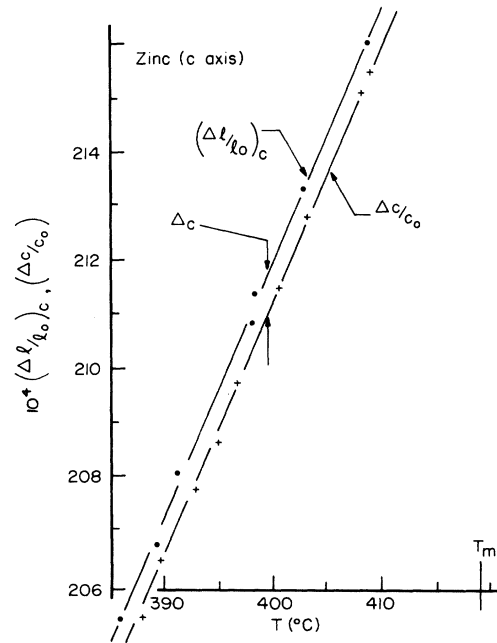


FIG. 3. Bulk (●) and lattice parameter (+) dilation in the c -axis direction in Zn at temperatures approaching the melting point.

lifetime saturates at $\sim 300^\circ\text{C}$, the lower limit for any measurable effect on the thermal expansion by the equilibrium vacancy concentration. However, the positron studies are sensitive to vacancy concentrations as small as 5×10^{-7} . At these levels, isolated single vacancy sites are the only significant point defect type. The positron annihilation experiments thus give unambiguous measures

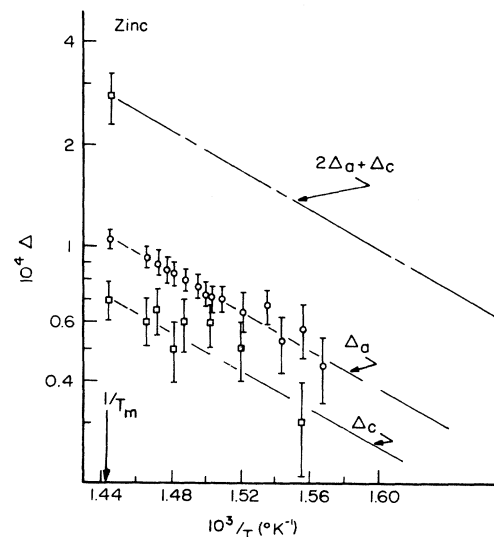


FIG. 4. Dilation differences, Δ_a and Δ_c , and vacancy fraction, $2\Delta_a + \Delta_c$, vs $1/T$ for Zn.

of the monovacancy formation energy. The continuation of the same value for E^f into the region of temperatures near the melting point used for thermal expansion measurements indicates that no major modification needs to be made in the analysis for the case of Zn to account for significant divacancy or higher-order vacancy groups.

The present result also agrees with the estimates made by Gilder and Wallmark¹¹ from their bulk expansion data and an "extrapolation" model of the "defect-free" lattice at high temperatures. Their result was $E^f = 0.50 \pm 0.05$ eV.

The present value for the vacancy-formation energy also agrees with a number of the common "rules of thumb". The activation energy for self diffusion in Zn is 0.95 eV,¹⁶ which is within the expected range (approximately twice the formation energy). The correlation with the melting temperature,¹⁷ $E^f \sim 9kT_m$, gives a value of 0.54 eV.

B. Entropy of formation

The entropies of formation in hexagonal metals (see Table III) are significantly smaller than entropies in cubic metals. The measured S^f values in fcc metals are spread over the range $(1-6)k$ and with a typical value of $1.5k$ (see a review of the data in Ref. 2). The predictions from theory are in the range of $(1.5-2.5)k$.¹⁸⁻²⁰ The results for S^f in hexagonal metals are in the range $(0-1)k$ with a typical value of $0.5k$.

An interesting consequence of the small values of S^f seen in hexagonal metals is suggested by the recent calculation of Brudnoy²⁰ for the harmonic perturbation of the lattice by vacancy formation. The general result (independent of lattice symmetry) for the harmonic case is $S^f = (\frac{1}{2}d)k$, where d is the dimensionality of the crystal (and thus, $S^f = 1.5k$ for a three-dimensional lattice). This harmonic result represents a lower limit to the perturbations of the band frequencies in the crystal. However, an entropy of formation much less than $1.5k$ could arise from the establishment of strong "out-of-band" localized modes associated with the vacancy site. The results for Zn, Cd, and Mg sug-

gest that these local-mode effects could play a major role in the lattice relaxations in these metals.

C. The strain ratio, Δ_a/Δ_c , and comparison with electromigration measurements

In vacancy-flux electromigration experiments, dimension changes are driven by vacancy (and compensatory mass) flow in the presence of a strong steady-state temperature gradient and axial dc current densities in the range of 10^4 amp/cm².²¹ For a cylindrical specimen, the dimension changes are used to calculate an isotropy factor α , which is the ratio of the longitudinal dimension changes (as measured by the displacement of inscribed surface markers) and the volume dilation (the sum of the longitudinal and twice the radial dimension changes). For a cubic material which is free of constraining stresses, the isotropy factor should be $\frac{1}{3}$. The important cases for comparison to thermal-expansion measurements are those electromigration measurements which are carried out on noncubic single-crystal specimens whose principal axes are oriented approximately parallel or perpendicular to the current flow. If the cylindrical specimen is large enough so that dislocation climb process dominates the equilibration of the vacancy population in the cooler regions on either side of the central-temperature maximum, then the ratio of the isotropy factors for specimens which are oriented perpendicular and parallel to the cylinder axis (and current flow), $\alpha_{\perp}/\alpha_{\parallel}$, should be analogous to the Δ_a/Δ_c ratio measured in thermal-expansion experiments.

The results for the axial metals for which dimensional changes have been measured by both thermal-expansion and electromigration methods are collected in Table IV. The ratio of the dimensional changes along the principal axis directions, δ_a/δ_c , is related to the observed isotropy ratio through

$$\frac{\alpha_{\perp}}{\alpha_{\parallel}} = \frac{\delta_c \cos^2 \psi_{\perp} + \delta_a \sin^2 \psi_{\perp}}{\delta_c \cos^2 \psi_{\parallel} + \delta_a \sin^2 \psi_{\parallel}}, \quad (6)$$

where ψ_{\perp} and ψ_{\parallel} are the angles between the principal axis (c) and the cylinder axis for perpendicular- and parallel-oriented specimens respectively.

Similar senses to the observed anisotropy are seen for comparisons between electromigration experiments and the thermal-expansion measurements in Zn (the present work), Mg,⁵ Cd,³ and⁶ Sn (where the dimensional changes are practically isotropic). The degree of anisotropy seen in the electromigration experiments is less than the observed values in thermal expansion by as much as ~30%. Surface stresses induced by the curvature

TABLE III. Entropies of formation for vacancies in hexagonal metals.

Metal	S^f/k	Reference
Zn	0.5 ± 0.3	This work
	1.1 ± 1.0	7
Cd	0.3 ± 0.4	3
	0.5 ± 0.1	4
Mg	0 ± 0.3	5

TABLE IV. Dislocation climb-induced strains in thermal expansion and electromigration experiments.

	Thermal-expansion data		δ_a/δ_c	Electromigration data		Reference
	Δ_a/Δ_c	Reference		$\langle\alpha_{\perp}/\alpha_{\parallel}\rangle$	$\psi_{\perp}/\psi_{\parallel}$	
Zinc	1.5 \pm 0.2	This work	1.3 \pm 0.1	1.22 \pm 0.05	75°/24°	22
	0.175	7				
Cadmium	0.43 \pm 0.2	3	0.66	0.77 \pm 0.05	62°/24°	23
	\sim 1 (temperature dependent)	4				
Magnesium	1.78 \pm 0.3	5	1.24 \pm 0.1	1.13 \pm 0.1	63°/22°	24
Tin	0.90 \pm 0.1 ^a	6	0.91 \pm 0.05	0.91 \pm 0.05	81°/9°	25

^aBy extrapolation of thermal dilation.

of the electromigration specimen profile can constrain the free dilation of the crystal and reduce the anisotropy of the observed strains.²⁶

However, measurements on small single-crystal cubes of Zn by Balzer⁷ indicate that the net strain arising from dislocation climb along the basal direction is nearly six times larger than the strains produced by dislocation climbing along the *c*-axis direction. This result for Δ_a/Δ_c is opposite in sense and much larger in magnitude than the present results and the electromigration work of Routhort.²² Using the same combination of interferometry and x-ray dilatometry in bct Sn, Balzer⁷ found the high-temperature vacancy fraction to be less than 3×10^{-5} . This vacancy fraction is an order of magnitude lower than the typical result for metals² and estimates of the vacancy fraction in Sn from quenched-resistivity data and thermal-expansion measurements.⁶

A similarly unresolved situation occurs in the experiments with Cd. The measurements by Feder and Nowick³ on specimens cut from a large single crystal indicated a larger dimensional change along the *c*-axis direction (corresponding to a larger net-strain effect from the climb of dislocations whose Burger's vectors have their largest component perpendicular to the basal plane). This is in agreement with the sense of $\delta_a/\delta_c < 1$ seen in the electromigration experiments of Alexander.²³ In comparison of results from separately grown crystals, Feder and Nowick found that the Δ_a/Δ_c ratio could be reversed in sense up to a value of 1.4. This led them to argue that the strain ratio, Δ_a/Δ_c , is in all cases sample dependent and that the important condition is the initial distribution of dislocation orientations which are frozen into the crystal matrix at solidification. The subsequent measurements of Janot and George⁴ also show a "specimen dependence" with strain ratios generally greater than unity. The strain ratios seen by Feder and Nowick are independent of temperature; which is consistent with diffusion-limited

climb¹⁰— although not to the exclusion of other more complex conditions. However, the strain ratios measured by Janot and George are strongly temperature dependent with the strain ratios derived from crystals grown perpendicular and parallel to the *c*-axis direction becoming more and less isotropic ($\Delta_a/\Delta_c = 1$), respectively, with increasing temperature. This suggests that the more general condition, where the strain ratio is dependent on the net jog formation rate (in general, temperature dependent) as well as the net distribution of dislocation orientations, exists for the case of Cd.

The difficulty in obtaining consistent results between different experiments, both for the sense and the temperature dependence of the strain ratio, is a consequence of the "black box" nature of both electromigration and thermal-expansion experiments. The first-order expression of Feder and Nowick¹⁰ for the strain ratio is

$$\frac{\Delta_a}{\Delta_c} = \frac{1 \sum N_i(T) \Lambda_i \sin^2 \psi_i}{2 \sum N_i(T) \Lambda_i \cos^2 \psi_i}, \quad (7)$$

where $N_i(T)$ is the number of vacancies generated per unit length while the temperature of the crystal is changed from $T_0 (\ll T_m)$ to T , Λ_i is the density of dislocations of type i and ψ_i is the angle between the *c* axis and a unit normal to the extra atom plane. The observed strain ratio is then a sum over all dislocation orientations and climb rates. Janot and George⁴ have noted the additional effect of vacancy generation from surface oxidation in Cd which can produce a difference between the observed net strains for heating and cooling cycles.

For the case of diffusion limited climb, the strain ratio reduces to

$$\frac{\Delta_a}{\Delta_c} = \frac{1 \sum \Lambda_i \sin^2 \psi_i}{2 \sum \Lambda_i \cos^2 \psi_i}. \quad (8)$$

Feder and Nowick assume that the distribution of dislocation orientations as well as the total num-

ber of dislocations is fixed by the solidification conditions. However, x-ray topography observations²⁷ in Al of the annealing of quench-formed dislocation loops show a rapid (~20 h) development of random dislocation arrays characteristic for a cubic structure at temperatures far removed from the melting point. Transmission electron microscopy of dislocations²⁸ in Zn and Cd display a wealth of climb and glide interactions between dislocations during the recovery from thermal and mechanical stress. These processes likewise can proceed at room temperature. The preliminary annealing and prolonged duration of high-temperature conditions which occur in thermal-expansion experiments should allow ample opportunity for similar dislocation motion and interaction and changes in the distribution of dislocation orientations from the initial conditions at solidification to a distribution which is characteristic of the specific material. If these "well-annealed" conditions were obtained then there should be complete agreement between the sense of the strain

ratios observed in electromigration and thermal-expansion experiments. The failure of the observations to agree on the sense or, in the example of Cd—where specific conclusions were made, the temperature dependence of the strain ratios indicates that very little can be said with certainty about dislocation climb processes in these noncubic metals from observations of the average climb-induced strains alone. One needs to have direct observations of the dislocation densities and specific climb rates under conditions which approximate those in the bulk crystal.

ACKNOWLEDGMENTS

Recognition is given to Dr. Ralph Feder and IBM-Yorktown Heights for the generous donation to RPI of the x-ray apparatus used in this work. We thank Dr. Balzer for sending us the results of his work in Zn and Sn prior to publication. The valuable assistance and advice of Dr. Lalit Chhabildas and Dr. H. B. Huntington are gratefully acknowledged.

*Work supported by NASA (NGL-33-018-003).

[†]Based on a thesis submitted to the Physics Department at Rensselaer Polytechnic Institute in partial fulfillment of the requirements for the Ph.D. degree.

[‡]Present address: Materials Science and Engineering, Bard Hall, Cornell University, Ithaca, N. Y. 14853.

[§]Present address: Laboratoire des Propriétés Mécaniques et Thermodynamiques des Matériaux, Université Paris-Nord, Villetaneuse, France, 93430.

¹R. Feder and A. Nowick, Phys. Rev. 109, 1959 (1958).

²For a review of the results of this work, see A. Franklin in *Point Defects in Solids*, edited by J. Crawford and L. Slifkin (Plenum, New York, 1972), Vol. I, p. 1.

³A. Nowick and R. Feder, Phys. Rev. B 5, 1244 (1972).

⁴C. Janot and B. George, Phys. Rev. B 12, 2212 (1975).

⁵C. Janot, D. Mallejac, and B. George, Phys. Rev. B 2, 3088 (1970).

⁶M. Current and L. Chhabildas (unpublished).

⁷R. Balzer (private communication).

⁸R. W. Balluffi and R. O. Simmons, J. Appl. Phys. 31, 2284 (1960).

⁹K. Fisher and H. Hahn, Z. Phys. 172, 172 (1963).

¹⁰A. S. Nowick and R. Feder, Phys. Rev. B 5, 1238 (1972).

¹¹H. M. Gilder and G. N. Wallmark, Phys. Rev. 182, 771 (1969).

¹²W. L. Bond, Acta Crystal. 13, 814 (1960).

¹³S. Apostolu, M. S. thesis (Rensselaer Polytechnic Institute, Troy, N. Y., 1970) (unpublished).

¹⁴B. D. Cullity, *Elements of x-Ray Diffraction* (Addison-Wesley, Reading, Mass., 1956).

¹⁵B. McKee, W. Triftshauser, and A. Stewart, Phys. Rev. Lett. 28, 358 (1972).

¹⁶A. P. Batra, Phys. Rev. 159, 487 (1967).

¹⁷Ref. 2, p. 27.

¹⁸H. B. Huntington, G. Shirn, and E. Wajda, Phys. Rev., 99, 1085 (1955).

¹⁹J. Burton, Phys. Rev. B 5, 2948 (1970).

²⁰D. Brudnoy, J. Phys. Chem. Solids 37, 1109 (1976).

²¹H. B. Huntington, *Diffusion*, edited by H. I. Aaronson, (ASM, Cleveland, 1973), p. 155.

²²J. Routbort, Phys. Rev., 176, 796 (1968).

²³W. Alexander, Z. Naturforsch. 26, 18 (1971).

²⁴J. Wohlgemuth, J. Phys. Chem. Solids 36, 1025 (1975).

²⁵A. Khosla, J. Phys. Chem. Solids 36, 395 (1975).

²⁶A. Lodding, J. Phys. Chem. Solids 26, 143 (1965).

²⁷B. Baudelet and G. Champier, Cryst. Lat. Def. 4, 95 (1973).

²⁸P. B. Price, *Electron Microscopy and Strength of Crystals*, edited by G. Thomas and J. Washburn (Wiley-Interscience, New York, 1963), p. 41-130.